Journal of Intelligent Systems and Internet of Things
Vol. 14, No. 01, PP. 293-304, 2025
DOI: https://doi.org/10.54216/JISIoT.140123

Deep Learning Driven LSTM with Spider Wasp Optimizer Algorithm for Frictional Force Based Landslides Prediction Model

Domi Evangeline . S[1,*], G. Usha[1]

[1]Department of Computing Technologies, SRM Institute of science and Technology, Kattankulathur, Chennai, India
Emails: domievangelinesundararaj@gmail.com; ushag@srmist.edu.in

Abstract

Landslides establish a main geologic threat of strong concern in many parts of the world. The vigor of soil, rocks, or other rubbish moving down a slope can destroy whatever in its track. Landslides happen in an extensive variety of geological and structural settings, geomechanical contexts, and as a response to numerous triggering and loading procedures. They are frequently related to other main natural disasters like floods, earthquakes, and volcanic waves. Landslides occasionally attack without noticeable warning. While only some cases have been examined the earlier, modern monitoring models are certain to deliver a wealth of novel quantitative observations based on SAR (synthetic aperture radar) and GPS technology for mapping the surface velocity area. This study emphasizes the latent of incorporating advanced machine learning (ML) models with geophysical data to improve prediction of landslides and risk management strategies. This study develops a Predicting Landslides with frictional-based Deep Learning using Spider Wasp Optimizer (PLFFDL-SWO) Method. The major intention of the PLFFDL-SWO technique lies in the robust frictional force based on predicting landslides. In the presented PLFFDL-SWO model, Z-score normalization is performed to transform the raw data into compatible format. Then, the long short-term memory (LSTM) model is utilized for the prediction of landslides. LSTM is a recurrent neural network (RNN) type, for predicting landslides based on frictional force data. Traditional landslide prediction methods often struggle with temporal dynamics and nonlinear relationships inherent in geophysical data. Finally, the spider wasp optimizer (SWO) algorithm is exploited for the optimal hyper parameter adjustment of the LSTM model to improve prediction accuracy. The experimentation result investigation of the PLFFDL-SWO technique can be examined by employing a benchmark dataset. The simulation outcomes reported the supremacy of the PLFFDL-SWO technique under different measures

Received: February 22, 2024 Revised: May 10, 2024 Accepted: August 14, 2024

Keywords: Landslide Prediction; Deep Learning; Spider Wasp Optimizer; Long Short-Term Memory; Frictional Force

1. Introduction

Landslides are universal in sloping environments and are handled by climatic, tectonic, or human actions [1]. Landslide accidents arise if the hazardous effort of rocks and soil indirectly or directly influences susceptible human infrastructure and settlements, on occasion producing extensive damages. Landslide threats can be intensified by environmental changes like growth in the magnitude or frequency of rainfall and glacial mass ruin [2]. Naturally, global agencies and organizations encourage landslide threat reduction strategies, which contain understanding risks and improving disaster preparation for actual response [3]. Several investigations on landslide reduction and prediction destruction of landslide damage are made. Nowadays, landslide hazard analysis and risk assessment have become a main topic in landslide studies and so, lots of new progress has been in those fields [4]. Particularly, the application of geospatial and information methods namely geographic information systems (GIS) and remotely sensed has prominently added to landslide hazard assessment analyses for several years [5].

Landslide hazard assessment, with hazard analysis and investigation, applies to identify and quantify illustrating the possible landslide hazards, and therefore, estimating the likelihood of incidence of landslides in a particular time [6].

A type of various techniques and methods for estimating landslide vulnerability are presented [7]. Various machine learning (ML) algorithms have recently been intended and applied to mapping vulnerability to landslides. These methods contain neuro-fuzzy, artificial neural networks (ANN), decision trees, random forests (RF), and support vector machine (SVM) algorithms. Recently, different hybrid methods have been also advanced by joining statistical models with ML approaches [8]. Among these hybrid approaches are greater than traditional algorithms. To control landslide vulnerability at the local level, this diverse practice is also used by the usage of remote sensing secondary or spatial data and is examined in the GIS atmosphere [9]. In recent years, numerous deep learning (DL) methods have also been applied to increase the accuracy of the landslide vulnerability modeling method, with the most important being the convolutional neural networks (CNNs) [10].

This study develops a Predicting Landslides with frictional-based Deep Learning using Spider Wasp Optimizer (PLFFDL-SWO) Method. The major intention of the PLFFDL-SWO technique lies in the robust frictional force based on predicting landslides. In the presented PLFFDL-SWO model, Z-score normalization is performed to transform the raw data into compatible format. Then, the LSTM model is utilized for the prediction of landslides. LSTM is a type of RNN, for predicting landslides based on frictional force data. Traditional landslide prediction methods often struggle with temporal dynamics and nonlinear relationships inherent in geophysical data. Finally, the spider wasp optimizer (SWO) algorithm is exploited for the optimal hyperparameter adjustment of the LSTM model to improve prediction accuracy. The experimentation result analysis of the PLFFDL-SWO approach is tested by using a benchmark dataset.

2. Related Works

Meng et al. [11] presented a new DL method, which integrates the LSCDBN the GWO algorithm, and the WOA, to implement landslide defencelessness evaluation. This method alleviates the challenges of feature fusion for constant input variables for landslide situation factors, inadequate landslide instances, and local targets in the training method. To enable this study, a particular compilation of present landslide incidences has been utilized to generate a database containing eighteen landslide naturalization factors. To equate the model performance, a group of statistical measures has been utilized. Alqadhi et al. [12] propose to improve the landslide prediction in the region of Saudi Arabia by combining DNNs, 1D CNNs, and an integrated DNN and CNN ensemble DCN with XAI methods. This XAI approach improves the understandability of these intricate DL methods, so enabling best decision-making tactics. In addition, the DNN method can be utilized to integrate the principles of game theory, evaluating the distinct effect of variables on landslide prediction. Xu et al. [13] propose the CAS Landslide Dataset, a multi-sensor and largescale dataset for DL-based landslide recognition, advanced by the AI Group at the Institution of Environment and Hill Dangers, CAS. The dataset goal is to tackle the challenges faced in landslide identification. With the upsurge in landslide incidences owing to earthquakes and weather changes. There is an increasing need for a comprehensive and precise dataset to help efficient and fast landslide identification.

Guerrero-Rodriguez et al. [14] developed an image dataset utilizing a legitimate landslide record that the author updated and verified based on newspaper data and analysis of study area satellite images. The images covering landslide peaks and the real generating values of the training factors at the feature level of (5×5 pixels). Our method concentrates on the particular position wherever the landslide initiates and its presence, unlike other workings, which consider the complete landslide region as the incidence of the happening. These images resemble anthropological, hydrological, geomorphological, and geological variables that have been loaded comparably to the channels of a traditional image to train and feed a CNN. Chen et al. [15] present a novel lightweight DL-based method, BisDeNet, for effectual LD. To enhance the efficacy of the presented BisDeNet. The author substituted the framework path in the original BiSeNet with DenseNet owing to its robust extraction of features capability, some vital parameters, and lower method difficulty. 2 locations with various and descriptive landslide changes are chosen as the research regions to authenticate the performance of our presented BisDeNet.

Ma and Mei [16] proposed a comprehensive landslide distortion predicting technique, which studies spatiotemporal relationships of landslide distortion by incorporating field knowledge into understandable DL. By spatially taking the connections among various distortions from various observing facts, our system gives the forecasting and understanding of landslide systematized behavior. By incorporating particular field knowledge related to every observance point and integrating interior properties with exterior variables. Yang et al. [17] present

a new multivariable landslide deposition prediction technique, which depends on graph DL and GNSS positioning. In initial method, the monitoring model graph structure depends on the GNSS monitoring points work locations and creates the graph node adjacency matrix. Then make the predicted and historical time series feature matrices by utilizing the processing temporal data containing GNSS dislocation, soil wetness, rainfall and graph structure, and the groundwater table.

3. Materials and Methods

In this study, we have advanced a new PLFFDL-SWO methodology. The main objective of the PLFFDL-SWO method lies in the robust frictional force based on predicting landslides. Figure 1 illustrates the entire procedure of PLFFDL-SWO method.

A. Z-score Normalization

Initially, the presented PLFFDL-SWO model undergoes Z-score normalization to transform the raw data into compatible format. The standard score (normally denoted as a z-score), is highly beneficial statistic because it (a) permits the programmer to compute the possibility of a score arising within our usual distribution and (b) permits equating dual scores that are from the dissimilar normal distribution [18]. This is completed by adapting (standardizing) scores in a normal distribution to z-score and converting a standard distribution of normal. Every value of input was normalized as per Eq. (1) as expressed below:

$$z(ij) = \frac{a(ij) - \mu}{\alpha} \tag{1}$$

Here, $z(ij)$ denotes a novel value; $a(ij)$ means an old value; μ refers to mean of the column; α indicates standard deviation; in $i = 1 - n$, the n refers to no. of inputs or rows; and in $j = 1 - k$, the k indicates the no. of bits, which signifies that every input is 32 bits.

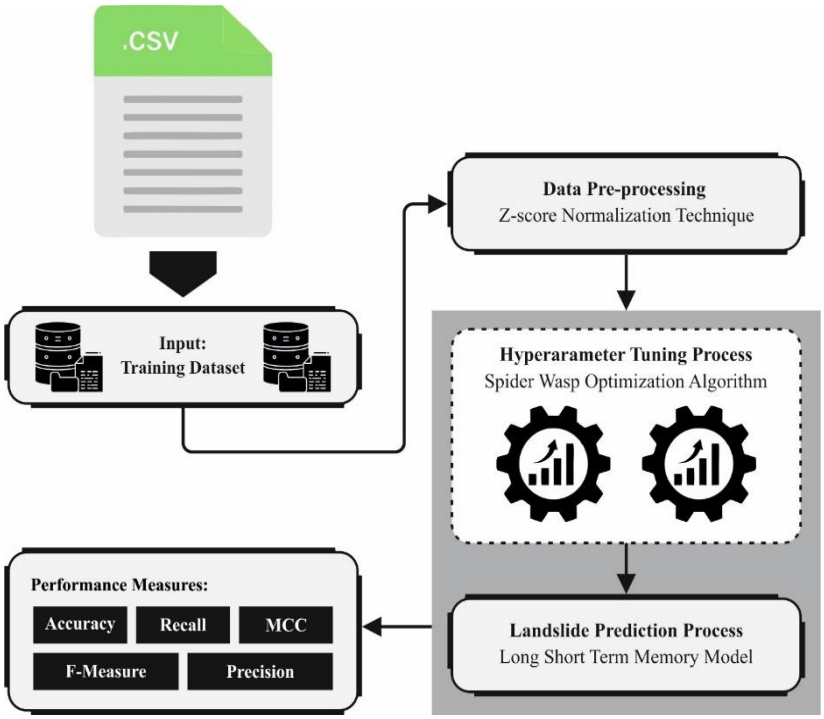

Figure 1. Overall process of PLFFDL-SWO model

B. LSTM Classifier

Then, the LSTM model is utilized for the prediction of landslides. The RNNs training method develops gradient vanishes difficulties [19]. RNNs are simply storing short-term information and have problems transmitting information for an extended time. They developed the LSTM as the solution. The advanced recurrent neural network (RNN) type is used in various areas for example: speech and handwriting recognition. LSTM is the architecture network that together with a proper gradient-based model can utilize memory gates and cells for storing information for a longer time. They identify that the cell state is the basis of the LSTM approach for the

state of the cell signifies the memory attribute. Easier, the state of a cell acts similar to a transport line, which stores and takes information. This information penetrating the state of a cell can be filtered in the gates. These gates consume the control to remove or add information from and to the state of a cell. There are 3 gates: input, output, and forgetting gates. The forgetting gates take input information approved from the prior hidden layer (HL), h_{t-1}, and the present input, x_t. Passed this input through a sigmoidal function, which reverts values amid 0 and 1, whereas 0 and 1 means nothing and everything goes through. This initial gated output f_t is:

$$f_t = \sigma\left[W_f(h_{t-1}, x_t) + b_f\right]. \quad (2)$$

The inputting gate selects that information to keep within the state of the cell. These gates contain dual portions. Primary, it obtains inputs h_{t-1} and x_t and permits them through a sigmoidal function in the following:

$$i_t = \sigma[W_i(h_{t-1}, x_t) + b_i]. \quad (3)$$

Afterward, it permits similar inputs through a hyperbolical tangent function, which makes a new vectored information:

$$\tilde{C}_t = \tanh[W_c(h_{t-1}, x_t) + b_c]. \quad (4)$$

The dual outputs, i_t and $\tilde{C}_t$ are added and combined to the cell state. The present period state of a cell can be generated with the outputs from the original and

$$C_t = f_t C_{t-1} + i_t \tilde{C}_t, \quad (5)$$

The output of forgetting gates, f_t, can be multiplied by the information passed from the preceding period state of the cell, C_{t-1}. Formerly, the result from the inputting gate, $i_t \tilde{C}_t$, can be additional, and the novel state of a cell, C_t was generated.

The outputting gate also gets inputs h_{t-1} and x_t and carries them through a sigmoidal activation. The output, o_t, can be represented below:

$$o_t = \sigma[W_o(h_{t-1}, x_t) + b_o]. \quad (6)$$

Meanwhile, the state of a cell, C_t, permits over a hyperbolical tangent function and the outputting has been multiplied with 0_t, to choose that information the novel HL, h_t, will transfer to the following time. This can be designated in the following:

$$h_t = o_t tanh[C_t], \quad (7)$$

It is obvious that the 3 sigmoidal functions, σ, and the hyperbolical tangent function, $tanh$, are directing the 3 gates. The scalar multiplication can be signified as $\times$ and addition can be represented as $+$. Generally, the LSTM upgrades the state of a cell, from C_{t-1} to C_t, filtering non-important and important information through the 3 gates, and creates h_t. Figure 2 depicts the structure of LSTM.

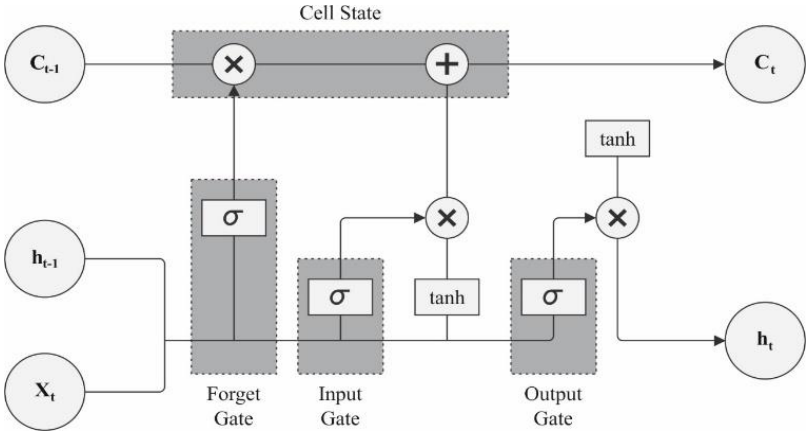

Figure 2. LSTM Architecture

C. Parameter Tuning

Finally, the SWO algorithm is exploited for the optimal hyperparameter adjustment of the LSTM model to improve prediction accuracy. SWO is a developed swarm optimizer technique, which represents what spider wasps (female) do while they search, construct nests, and mate [20]. At first, search behavior's main intention is food and getting

the appropriate spider for larval growth. Next, building nest imitators is the model of drawing the victim to the layers with a proper dimension for the prey and egg. Then, mate behavior imitates the features of the offspring built by inlaying the egg using the even crossover operator. Thus, the below mentioned are the sub-sections, which deliver a numerical method of these behaviors.

Initial population, every spider wasp is considered a solution in the present group. Eq. (8) displays the vector of N-dimension.

$$\overrightarrow{SpW} = [p_1, p_2, \dots, p_N] \tag{8}$$

A random population contains M vectors, which are produced among the pre-defined ub (upper bound) and lb (lower bound) utilizing Eq. (9).

$$SpW_{popu} = \begin{bmatrix} spw_{1,1} & spw_{1,2} & spw_{1,3} & \dots & spw_{1,N} \\ spw_{2,1} & spw_{2,2} & spw_{2,3} & \dots & spw_{2,N} \\ \vdots & \vdots & \vdots & \vdots & \vdots \\ spw_{M,1} & spw_{M,2} & spw_{M,3} & \dots & spw_{M,N} \end{bmatrix}, \tag{9}$$

Whereas, SpW_{popu} denotes the early population. Eq. (3) is utilized to generate any random solution.

$$\overrightarrow{SpW_p^g} = \overrightarrow{lb} + \overrightarrow{rand} \times \left(\overrightarrow{ub} - \overrightarrow{lb}\right), \tag{10}$$

Here, g specifies the indices of present group, and p denotes the population index ($p = 1{,}2\ M$). $\overrightarrow{rand}$ indicates a vector of N-size that ranges between 0 and 1.

Exploration stage:

At this stage, the spider wasp hunts the search zone at random to get the prey. The mathematical formulation of this model is given below:

$$\overrightarrow{SpW_p^{g+1}} = \overrightarrow{SpW_p^g} + const_1 * \left(\overrightarrow{SpW_X^g} - SpW_y^g\right), \tag{11}$$

Whereas, $\overrightarrow{SpW_p^{g+1}}$ denotes the upgraded location of every female wasp with a constant motion ($const_l$) over the present direction. g represents the index of present generation, and p indicates the population index ($p = l, 2, \dots, M$). SpW_X^g and SpW_y^g are dual arbitrary solutions that are employed to classify the way of exploration. x and y denote their indices. The $const_1$ formulation is given below:

$$const_1 = |rand_{norm}| * rand_1, \tag{12}$$

Whereas, $rand_{norm}$ is a randomly produced number, which follows the normal distribution, $rand_1$ directs a number between 0 and 1 at random.

$$\overrightarrow{SpW_p^{g+1}} = \overrightarrow{SpW_{curr}^g} + const_2 * \left(\overrightarrow{lb} + \overrightarrow{rand_2} * \left(\overrightarrow{ub} - \overrightarrow{lb}\right)\right), \tag{13}$$

Whereas, $\overrightarrow{SpW_{curr}^g}$ denotes a randomly nominated solution. $const_2$ is a constant motion, and $rand_1$ specifies a randomly produced number among 0 and 1. lb and ub denote the lower and upper bound, correspondingly. $const_2$ is calculated utilizing Eq. (14).

$$const_2 = \frac{1}{1 + e^{lr}} * cos(2\pi lr), \tag{14}$$

where lr refers to the randomly produced number among 1 and -2.

Eqs. (11) and (13) are employed mutually to discover the search areas and the most supporting sites. Finally, the selection among these formulations is to yield the upgraded site for the female wasp as defined in Eq. (15).

$$\overrightarrow{SpW_p^{g+1}} = \begin{cases} Equation\ 4\ rand_3 < rand_4 \\ Equation\ 6\ otherwise\ ' \end{cases} \tag{15}$$

Here, $rand_3$ and $rand_4$ denotes the randomly produced numbers in [0,1].

Exploitation and exploration stage:

After discovering the prey, the spider wasp tries to find and destroy it. Generally, dual scenarios are accessible. The 1st situation is that spider wasps follow the target to hook and put in their nests. These situations can be demonstrated in Eq. (16). The 2nd scenario is that the wasp cannot able to get the released target. Eq. (18) shows this approach, and the tradeoff among those settings is achieved at random, as expressed in Eq. (20).

$$\overrightarrow{SpW_p^{g+1}} = \overrightarrow{SpW_p^g} + C * \left|\overrightarrow{rand_5} * \overrightarrow{SpW_X^g} - \overrightarrow{SpW_p^g}\right|, \quad (16)$$

Whereas g denotes the index of present generation, p represents the population index, SpW_X^g is a random solution, and x signifies its index. $\overrightarrow{rand_5}$ refers to a vector of randomly formed values within the limit [0,1]. C denotes a distance control parameter. Eq. (17) is employed to calculate C.

$$C = \left(2 - 2 * \left(\frac{p}{p_{\max}}\right)\right) * rand_6, \quad (17)$$

Here, $p_{\max}$ specifies the maximum generation, and $rand_6$ represents a randomly formed value in the range of [0,1]. C refers to a distance control parameter.

During the 2nd setting, the distance between the prey and the spider wasp slowly increases. This stage of exploitation is changed into exploration.

$$\overrightarrow{SpW_p^{g+1}} = \overrightarrow{SpW_p^g} * \overrightarrow{vec}, \quad (18)$$

Whereas, $\overrightarrow{vec}$ shows a vector, its values among v and -v. Eq. (19) calculates the v value that follows the normal distribution.

$$v = 1 - \left(\frac{p}{p_{\max}}\right), \quad (19)$$

$$\overrightarrow{SpW_p^{g+1}} = \begin{cases} Eq.(16)\ rand_3 < rand_4 \\ Eq.(18)\ otherwise\ ' \end{cases} \quad (20)$$

The algorithm uses the subsequent (tracking) and escaping tools to discover and utilize the area near the present wasps. Finally, the balance amid both phases is modified depending upon Eq. (21).

$$\overrightarrow{SpW_p^{g+1}} = \begin{cases} Eq.(22) & rand_p < v \\ Eq.(20) & otherwise' \end{cases} \quad (21)$$

Whereas, $rand_p$ designates a randomly formed integer in the range of 0 and 1.

Exploitation stage:

The Eq. (22) involves dragging the spider near the region and optimum position for nest-building.

$$\overrightarrow{SpW_p^{g+1}} = \overrightarrow{SpW^*} + cos(2\pi lr) * \left(\overrightarrow{SpW^*} - \overrightarrow{SpW_p^g}\right), \quad (22)$$

Here, $\overrightarrow{SpW^*}$ represents the optimum solution.

The 2nd formulation targets to make a spider's nest at the site of one female spider nominated at random. This calculation is expressed below:

$$\overrightarrow{SpW_p^{g+1}} = \overrightarrow{SpW_X^g} + rand_3 * |\wp| * \left(\overrightarrow{SpW_X^g} - \overrightarrow{SpW_p^g}\right)$$

$$+(1 - rand_3) * \vec{y} * \left(\overrightarrow{SpW_y^g} - \overrightarrow{SpW_z^g}\right), \quad (23)$$

Whereas $rand_3$ denotes a produced value inside the interval of 0 and 1 at random. $\wp$ is defined by a model named "levy flight, y, and x are indexed, which signify 3 solutions at random. $\vec{y}$ is a binary vector. Finally, $\vec{y}$ is intended utilizing Eq. (24).

$$\vec{V} = \begin{cases} 1\ \overrightarrow{rand_4} > \overrightarrow{rand_5} \\ 0\ otherwise \end{cases} \quad (24)$$

While $\overrightarrow{rand_4}$ and $\overrightarrow{rand_5}$ represent dual two vectors signifying randomly formed numbers in limit of [0,1].

As per the formulation set in Eq. (25), the Eqs. (22) and (23) are swapped in a random method.

$$\overrightarrow{SpW_p^{g+1}} = \begin{cases} Eq.(22)\ rand_3 < rand_4 \\ Eq.(23)\ otherwise\ ' \end{cases} \quad (25)$$

Finally, the balancing among the outlooks of pursuing target and nesting is over Eq. (26).

$$\overrightarrow{SpW_p^{g+1}} = \begin{cases} Eq.(21)\ p < M * v \\ Eq.(25)\ otherwise' \end{cases} \quad (26)$$

Mating behavior

The spider wasps have the aptitude to identify gender that is predictable by the size of host where an egg is placed. Smaller and bigger spider wasps specify male and female offspring, respectively. In this model, all spider wasps state a probable solution. Eq. (27) is employed to make these spider wasp eggs.

$$\overrightarrow{SpW_p^{g+1}} = Crossover\left(\overrightarrow{SpW_p^g}, \overrightarrow{SpW_m^g}, CrRa\right), \qquad (27)$$

Whereas, $Crossover$ refers to an operator, which is employed to achieve uniform crossover. The $\overrightarrow{SpW_p^g}$ and $\overrightarrow{SpW_m^g}$ resemble the female and male spider wasps, correspondingly. The SWO model produces male spider wasps, which are separate from female wasps utilizing Eq. (28).

$$\overrightarrow{SpW_m^{g+1}} = \overrightarrow{SpW_p^g} + \rightarrow e^l * |B| * \overrightarrow{vec_1} + (1 - e^l) * |B_1| * \overrightarrow{vec_2}, \qquad (28)$$

Whereas B and B_1 are dual-generated values at random. e refers to the exponential constant. Moreover, the formulation contains the set of vectors $\overrightarrow{vec_1}$ and $\overrightarrow{vec_2}$, which are computed utilizing the subsequent equations:

$$\overrightarrow{vec_1} = \begin{cases} \overrightarrow{x_a} - \overrightarrow{x_\iota} \, f(\overrightarrow{x_a}) < f(\overrightarrow{x_a}) \\ \overrightarrow{x_\iota} - \overrightarrow{x_b} \; otherwise \end{cases}, \qquad (29)$$

$$\overrightarrow{vec_1} = \begin{cases} \overrightarrow{x_b} - \overrightarrow{x_c} f(\overrightarrow{x_b}) < f(\overrightarrow{x_c}) \\ \overrightarrow{x_c} - \overrightarrow{x_b} \; otherwise \end{cases}, \qquad (30)$$

Where $a, b,$ and c are different from each other.

Decrease the size of population and preserve the memory

The length of the current population in every assessment is attuned utilizing the below-given calculation:

$$M = M_{\min} + (M - M_{\min}) \times v, \qquad (31)$$

Here, minimum population size is denoted by $M_{\min}$

The SWO model develops a fitness function (FF) to gain better performance classification. It controls a positive value to characterize the superior performance of the candidate solutions. In this work, the minimization of the classification rate of error can be determined by the FF, as specified in Eq. (32).

$$fitness(x_i) = ClassifierErrorRate(x_i)$$
$$= \frac{no\ of\ misclassified\ samples}{Total\ no\ of\ samples} * 100 \qquad (32)$$

4. Results Analysis and Discussion

The performance assessment of the PLFFDL-SWO model is examined using benchmark dataset [21]. The dataset comprises 1212 samples under 2 class labels as illustrated in Table 1. The total feature counts are 12 like Aspect, Curvature, Earthquake, Elevation, Flow, Lithology, NDVI, NDWI, Plan, Precipitation/Soil Moisture, Profile, and Slope.

Table 1: Details on Dataset

Class	No. of Samples
Normal	606
Landslide	606
Total Samples	1212

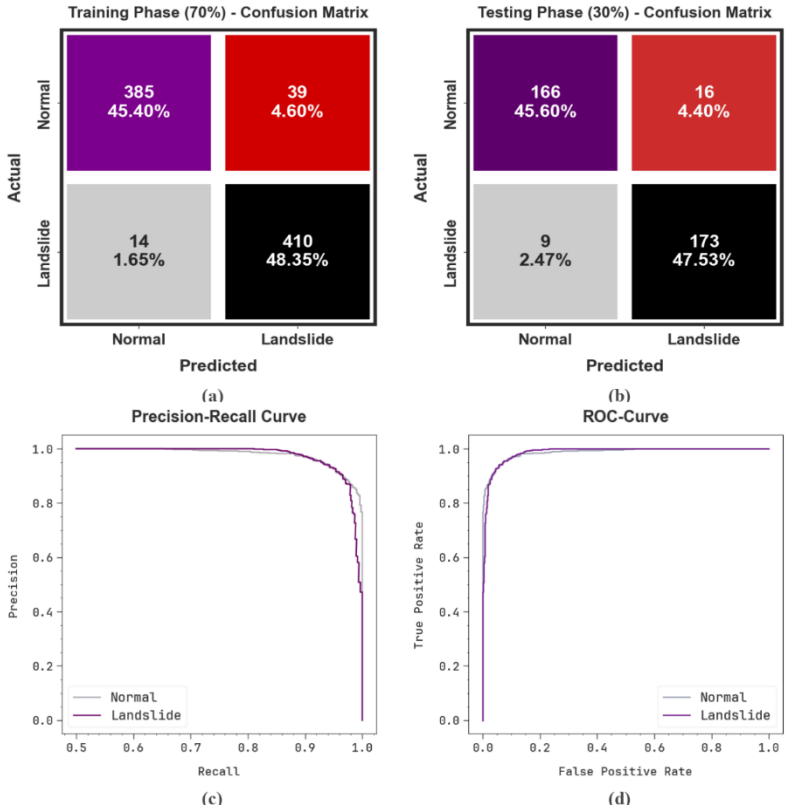

Figure 3. Classifier outcomes of (a-b) 70%TRAP and 30%TESP of confusion matrices and (c-d) PR and ROC curves

Figure 3 presents the classifier performance of the PLFFDL-SWO approach under the test database. Figures. 3a-3b demonstrates the confusion matrix with correct identification and classification of every dual class on a 70:30 TRAP/TESP. Figure 3c shows the analysis of PR, representing greater performance through each class label. Finally, Figure 3d demonstrates the analysis of ROC, indicating efficient outcomes with better values of ROC for different classes.

Table 2 and Figure 4 depict the classifier results of the PLFFDL-SWO model under 70%TRAP and 30%TESP. These values described that the PLFFDL-SWO technique appropriately recognized each sample. With 70%TRAP, the PLFFDL-SWO method provides average $accu_y$, $prec_n$, $reca_l$, $F_{measure}$ and MCC of 93.75%, 93.90%, 93.75%, 93.74%, and 87.65%, individually. Simultaneously, With 30%TESP, the PLFFDL-SWO system gives average $accu_y$, $prec_n$, $reca_l$, $F_{measure}$ and MCC of 93.13%, 93.20%, 93.13%, 93.13%, and 86.33%, respectively.

Table 2: Classifier outcome of PLFFDL-SWO technique under 70%TRAP and 30%TESP

Class	$Accu_y$	$Prec_n$	$Reca_l$	$F_{measure}$	MCC
TRAP (70%)					
Normal	90.80	96.49	90.80	93.56	87.65
Landslide	96.70	91.31	96.70	93.93	87.65
Average	93.75	93.90	93.75	93.74	87.65
TESP (30%)					
Normal	91.21	94.86	91.21	93.00	86.33
Landslide	95.05	91.53	95.05	93.26	86.33
Average	93.13	93.20	93.13	93.13	86.33

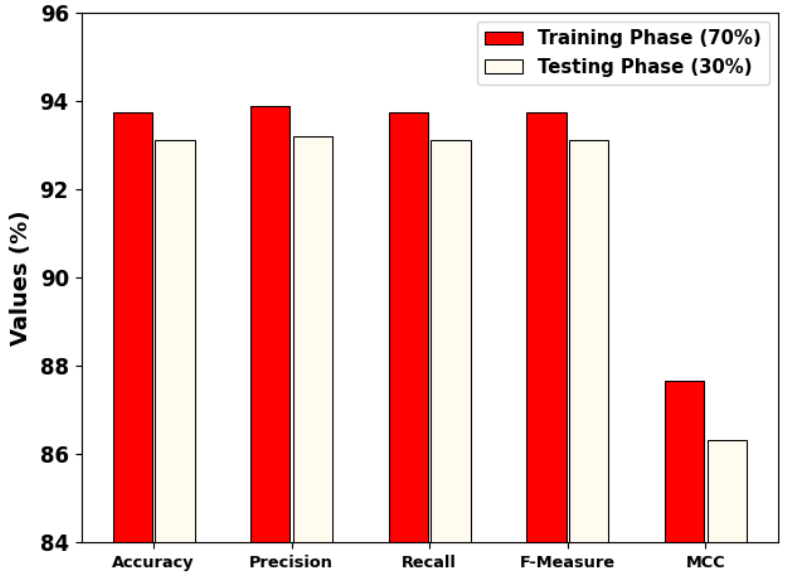

Figure 4. Average of PLFFDL-SWO technique under 70%TRAP and 30%TESP

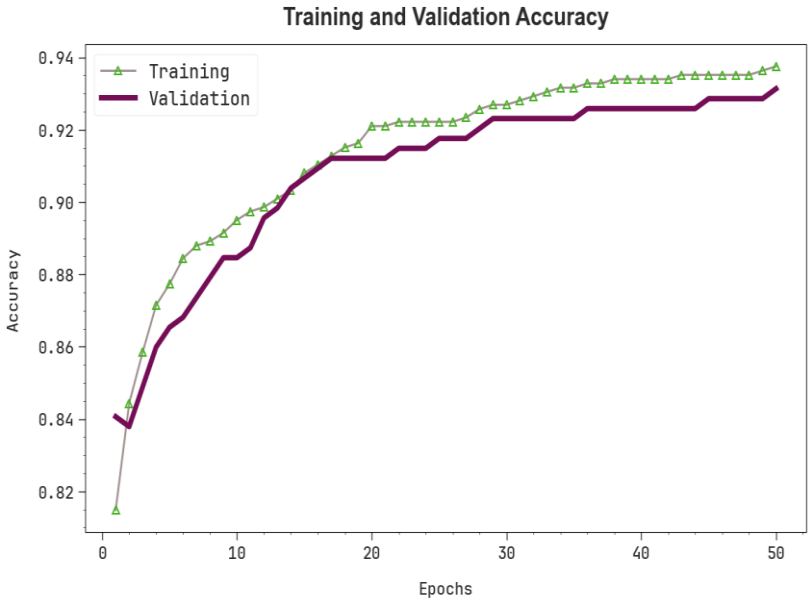

Figure 5. $Accu_y$ Curve of PLFFDL-SWO technique

In Figure 5, the training (TRA) and validation (VLA) accuracy values of the PLFFDL-SWO technique are portrayed. The correct performances are calculated for 0-50 number of epochs. The figure underlined that the TRA and VLA accuracy performances show an increasing tendency that informed the capacity of the PLFFDL-SWO approach with higher value across different numbers of iterations. Furthermore, the TRA and VLA accuracy stay nearer across the number of epochs that stated lower least overfitting and demonstrate the superior outcome of the PLFFDL-SWO technique, assuring steady prediction on unseen instances.

In Figure 6, the TRA and VLA loss graph of the PLFFDL-SWO methodology has been described. The loss values are calculated above an interval of 0-50 epoch counts. It can be signified that the TRA and VLA accuracy results designate a reducing trend, notifying the capacity of the PLFFDL-SWO system to balance a trade-off between data fitting and generalization. The steady decline in loss outcomes moreover assurances the better outcomes of the PLFFDL-SWO technique and tuning the prediction performances at the time.

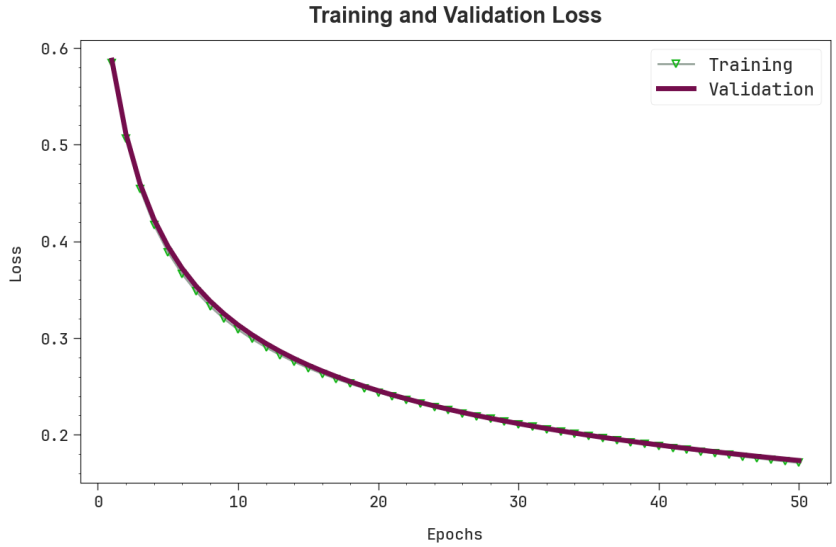

Figure 6. Loss curve of PLFFDL-SWO technique

Table 3 and Figure 7 inspect the comparative results of the PLFFDL-SWO approach with the recent techniques [22, 23]. The results underscored that the CNN-SVM, RF, LR, CNN, and SVM approaches have described poor performance. In the meantime, XGBoost, and AdaBoost systems have gained adjacent outcomes. Additionally, the PLFFDL-SWO process stated superior performance with higher $accu_y$, $prec_n$, $reca_l$, $and\ F_{measure}$ of 93.75%, 93.90%, 93.75% and 93.74%, correspondingly.

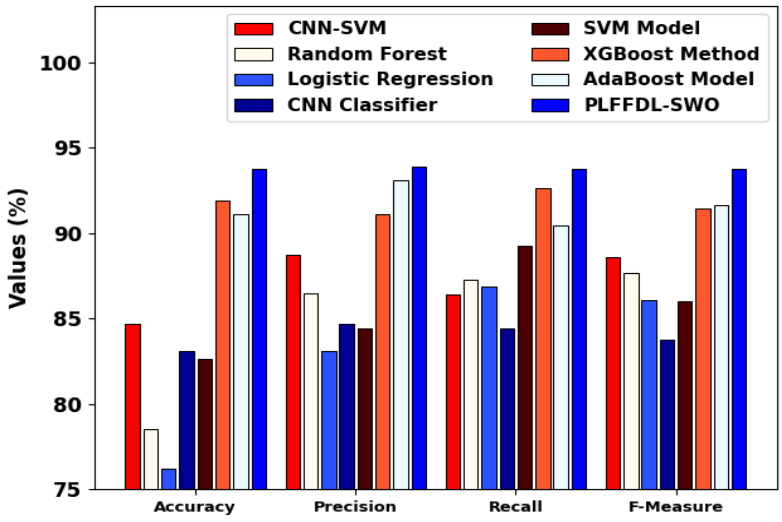

Figure 7. Comparative analysis of PLFFDL-SWO technique with existing models

Table 3: Comparative analysis of PLFFDL-SWO technique with existing models

Methods	Accuracy	Precision	Recall	F-Measure
CNN-SVM	84.69	88.71	86.42	88.60
Random Forest	78.50	86.47	87.30	87.68
Logistic Regression	76.20	83.08	86.87	86.06
CNN Classifier	83.10	84.67	84.44	83.77
SVM Model	82.61	84.43	89.25	86.01
XGBoost Method	91.90	91.13	92.61	91.42
AdaBoost Model	91.12	93.11	90.43	91.65
PLFFDL-SWO	93.75	93.90	93.75	93.74

5. Conclusion

In this study, we have established a new PLFFDL-SWO methodology. The main objective of the PLFFDL-SWO model lies in the robust frictional force based on predicting landslides. In the presented PLFFDL-SWO model, Z-score normalization is performed to transform the raw data into compatible format. Then, the LSTM model is utilized for the prediction of landslides. LSTM is a type of RNN, for predicting landslides based on frictional force data. Traditional landslide prediction methods often struggle with temporal dynamics and nonlinear relationships inherent in geophysical data. Finally, the SWO algorithm is exploited for the optimal hyperparameter adjustment of the LSTM model to improve prediction accuracy. The experimentation result investigation of the PLFFDL-SWO method can be examined by employing a benchmark dataset. The simulation outcomes reported the supremacy of the PLFFDL-SWO technique under different measures.

Funding: "This research received no external funding"

Conflicts of Interest: "The authors declare no conflict of interest."

References

[1] Peng L et al (2014) Landslide susceptibility mapping based on rough set theory and support vector machines: A case of the Three Gorges area, China. Geomorphology 204:287–301

[2] Gabet, E.A., 2007. Theoretical model coupling chemical weathering and physical erosion in landslide-dominated landscapes. Earth. Planet. Sci. Lett. 264, 259–265.

[3] Wang Y et al (2019) Comparison of convolutional neural networks for landslide susceptibility mapping in Yanshan County, China. Sci Total Environ 666:975–993

[4] Galli, M., Ardizzone, F., Cardinali, M., Guzzetti, F., Reichenbach, P., 2008. Comparing landslide inventory maps. Geomorphology 94, 268–289.

[5] Erener, A., Duzgun, H.S.B., 2010. Improvement of statistical landslide susceptibility mapping by using spatial and global regression methods in the case of More and Romsdal (Norway). Landslides 7, 55–68

[6] Wang Y et al (2020) Comparative study of landslide susceptibility mapping with different recurrent neural networks. Comput Geosci 138:104445

[7] Gariano, S.L., Sarkar, R., Dikshit, A., Dorji, K., Brunetti, M.T., Peruccacci, S., Melillo, M., 2019. Automatic calculation of rainfall thresholds for landslide occurrence in Chukha Dzongkhag, Bhutan. Bull. Eng. Geol. Environ. 78, 4325–4332

[8] Pham BT et al (2017) Hybrid integration of Multilayer Perceptron Neural Networks and machine learning ensembles for landslide susceptibility assessment at Himalayan area (India) using GIS. CATENA 149:52–63.

[9] Shou K-J, Lin J-F (2016) Multi-scale landslide susceptibility analysis along a mountain highway in Central Taiwan. Eng Geol 212:120–135.

[10] Al-Najjar, H.A.H., Pradhan, B., Kalantar, B., Sameen, M.I., Santosh, M., Alamri, A., 2021. Landslide susceptibility modeling: an integrated novel method based on machine learning feature transformation. Remote Sens. 13, 3281.

[11] Meng, S., Shi, Z., Li, G., Peng, M., Liu, L., Zheng, H. and Zhou, C., 2024. A novel deep learning framework for landslide susceptibility assessment using improved deep belief networks with the intelligent optimization algorithm. Computers and Geotechnics, 167, p.106106.

[12] Alqadhi, S., Mallick, J. and Alkahtani, M., 2024. Integrated deep learning with explainable artificial intelligence for enhanced landslide management. Natural Hazards, 120(2), pp.1343-1365.

[13] Xu, Y., Ouyang, C., Xu, Q., Wang, D., Zhao, B. and Luo, Y., 2024. CAS Landslide Dataset: A Large-Scale and Multisensor Dataset for Deep Learning-Based Landslide Detection. Scientific Data, 11(1), p.12.

[14] Guerrero-Rodriguez, B., Garcia-Rodriguez, J., Salvador, J., Mejia-Escobar, C., Cadena, S., Cepeda, J., Benavent-Lledo, M. and Mulero-Perez, D., 2024. Improving landslide prediction by computer vision and deep learning. Integrated Computer-Aided Engineering, 31(1), pp.77-94.

[15] Chen, T., Gao, X., Liu, G., Wang, C., Zhao, Z., Dou, J., Niu, R. and Plaza, A., 2024. BisDeNet: A new lightweight deep learning-based framework for efficient landslide detection. IEEE Journal of Selected Topics in Applied Earth Observations and Remote Sensing.

[16] Ma, Z. and Mei, G., 2024. Forecasting landslide deformation by integrating domain knowledge into interpretable deep learning considering spatiotemporal correlations. Journal of Rock Mechanics and Geotechnical Engineering.

[17] Yang, C., Yin, Y., Zhang, J., Ding, P. and Liu, J., 2024. A graph deep learning method for landslide displacement prediction based on global navigation satellite system positioning. Geoscience Frontiers, 15(1), p.101690.

[18] Al-Faiz, M.Z., Ibrahim, A.A. and Hadi, S.M., 2018. The effect of Z-Score standardization (normalization) on binary input due the speed of learning in back-propagation neural network. Iraqi Journal of Information and Communication Technology, 1(3), pp.42-48.

[19] Zitti, M., 2024. Forecasting salmon market volatility using long short-term memory (LSTM). Aquaculture Economics & Management, 28(1), pp.143-175.

[20] Osama, S., Ali, A.A. and Shaban, H., 2024. Gene selection based on recursive spider wasp optimizer guided by marine predators algorithm. Neural Computing and Applications, pp.1-18.

[21] https://www.kaggle.com/datasets/adizafar/landslide-prediction-for-muzaffarabadpakistan

[22] Aslam, B., Zafar, A. and Khalil, U., 2021. Development of integrated deep learning and machine learning algorithm for the assessment of landslide hazard potential. Soft Computing, 25(21), pp.13493-13512.

[23] Saha, S., Bera, B., Shit, P.K., Sengupta, D., Bhattacharjee, S., Sengupta, N., Majumdar, P. and Adhikary, P.P., 2023. Modelling and predicting of landslide in Western Arunachal Himalaya, India. Geosystems and Geoenvironment, 2(2), p.100158.